Proceedings of the ASME/JSME 2011 8th Thermal Engineering Joint Conference
AJTEC2011
March 13-17, 2011, Honolulu, Hawaii, USA

AJTEC2011-44493

AN EXPERIMENTAL STUDY OF HEAT TRANSFER FROM SMALL HORIZONTAL CYLINDERS AT NEAR-CRITICAL PRESSURES

Yohann Rousselet, Gopinath R. Warrier[1] and Vijay K. Dhir
University of California, Los Angeles, Henry Samueli School of Engineering and Applied Science
Mechanical and Aerospace Engineering Department
Henry Samueli School of Engineering and Applied Science
Los Angeles, CA, USA
[1]Contact Author

ABSTRACT

An experimental study of the free convection heat transfer from horizontally held wires to carbon dioxide at near-critical pressures has been performed. In the experiments, platinum wires of 25.4 μm, 76.2 μm and 100 μm, as well as a 101.6 μm diameter nichrome 60/20 wire were used. The pressure (P) and bulk temperature (T_b) of the fluid were varied in the range: 6.34 MPa ≤ P ≤ 9.60 MPa and 10 °C ≤ T_b ≤ 33.3 °C, respectively. Visual observation of the flow was realized using a high speed camera. The bulk fluid temperature is introduced as a new reference temperature for the calculation of fluid properties. Correlations were developed to predict the natural convection heat transfer rate at both subcritical and supercritical pressures. The correlations developed predict almost all the experimental data from the current study and those reported in the literature to within ± 15 %. No bubble-like flow pattern was observed for both platinum and nichrome wires.

NOMENCLATURE

C	constant, Eq. (10)
c_p	specific heat at constant pressure J/kgK
ΔT	temperature difference $T_w - T_b$, K
D	wire diameter, m
g	acceleration due to gravity, m/s^2
Ga	Galileo Number, Ga = gD^3 / ν^2
Gr	Grashof Number, Eq. (3)
h	heat transfer coefficient, W/m^{2}K
i	enthalpy, J/kg
k	thermal conductivity, W/mK
m	exponent, Eq. (10)
Nu	Nusselt Number, Nu = hD / k
P	pressure, Pa
Pr	Prandtl Number, Pr = μc_p / k
q	heat flux, W/m^2
Ra	Rayleigh Number, Ra = GrPr
T	temperature, K

Greek symbols

β	coefficient of thermal expansion, 1/K
μ	dynamic viscosity, Pa.s
ν	kinematic viscosity, m^2/s
ρ	density, kg/m^3

Subscripts

b	at bulk conditions
c	at critical state
i	integrated mean value
f	at film temperature, $T_f = (T_w + T_b) / 2$
p	at constant pressure
pc	at pseudocritical conditions
r	reduced (property/property at critical state)
ref	at reference state
sat	at saturation
w	at wall temperature

INTRODUCTION

In recent years, the interest in heat transfer to fluids at near-critical conditions has increased dramatically. This is due to the rise in the number of industrial applications using fluids at near-critical pressures, which are motivated by the desirable properties they exhibit. Consequently, the need for a better understanding of the heat transfer phenomena at these conditions has also increased.

The majority of the heat transfer studies to fluids at supercritical pressures have focused on forced convection in channels, and have been reviewed by Pioro *et al.* [1]. On the other hand, relatively few studies have focused on natural convection heat transfer. Some of the earliest experimental work on heat transfer to carbon dioxide at near critical pressures was performed by Knapp and Sabersky [2], Goldstein and Aung [3], and Grigull and Abadzic [4]. Grigull and Abadzic studied heat transfer at subcritical pressures, whereas Goldstein and Aung, along with Knapp and Sabersky, only studied natural convection heat transfer at supercritical pressures. Bubble-like

flow patterns were first reported by Griffith and Sabersky [5], and later by Knapp and Sabersky. Abadzic and Goldstein [6] did not notice any bubble-like activity. Nishikawa *et al.* [7] and Hahne and Neumann [8] studied the relation between the bubble-like flow and the heater material. The appearance of the bubble-like activity was reportedly followed by a sharp increase in the heat transfer coefficient (h). These studies concluded that the appearance of this flow pattern depended directly on the geometry and material of the heating surface, as well as fluid properties.

Hahne [9] performed experiments using platinum wires ranging in size from 50 μm to 300 μm in supercritical carbon dioxide. He found that the heat transfer coefficient showed a sharp increase with pressure (P) close to the critical pressure (P_c = 7.3773 MPa for CO_2). Also, it was shown that there is a sharp increase in h when the heater wall temperature (T_w) is close to the critical temperature (T_c = 30.978 °C for CO_2) or the pseudocritical temperature (T_{pc}, also called the transposed critical temperature). The pseudocritical temperature is defined as the temperature at which the specific heat capacity (c_p) reaches its maximum, for a given supercritical pressure. The heat transfer coefficient decreased when $T_w > T_{pc}$. The observed behavior was attributed to the large variations of the fluid property close to T_c and/or T_{pc}. The specific heat at constant pressure, for example, becomes infinite at the critical point. When P increases ($P > P_c$), the same behavior is observed at the T_{pc} corresponding to P. To illustrate this, Fig. 1 shows the variation of some thermodynamic properties of CO_2 with temperature at P = 8.10 MPa (T_{pc} = 35.25 °C).

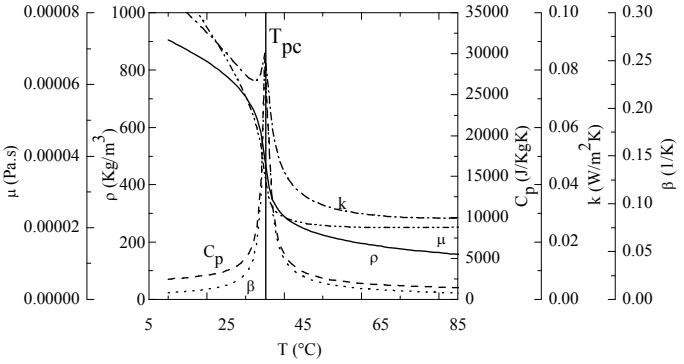

FIGURE 1. SOME PROPERTIES OF CARBON DIOXIDE AT P = 8.10 MPa

Relatively few correlations have been proposed for free convection heat transfer at near-critical pressures. However, none of them give satisfactory results. A major reason for this is the fact that there is no consensus with regards to the temperature at which the fluid properties are to be evaluated, and how these property variations are to be accounted for.

The lack of understanding of natural convection in fluids close to critical conditions is limiting our ability to design and develop systems that operate at these conditions. Hence there is a need to better understand the fundamentals of natural convection heat transfer at these conditions.

This study was designed to address some of these issues. The goal of the present investigation is to further our basic understanding of heat transfer phenomena at near-critical pressures and to extend the experimental database. Based on the experimental data we hope to develop accurate correlations for free convection heat transfer to carbon dioxide at near-critical conditions. A numerical study of natural convection heat transfer at near-critical pressures was simultaneously conducted. This is described in [10].

EXPERIMENTAL APPARATUS

The experimental apparatus consists of a horizontal wire mounted in a high pressure cylindrical stainless steel 316 vessel. The inner dimensions of the vessel are 100 mm in height and 41.3 mm in diameter, and the outer dimensions of the vessel are 254 mm in height and 150 mm in diameter. In order to enable visual observation, four single-crystal sapphire windows are provided on the high pressure vessel. The diameter of these windows is 38.1 mm. Visualization of the phenomenon was accomplished using a high speed (Fastec HR) camera. A schematic of the experimental apparatus is shown in Fig. 2.

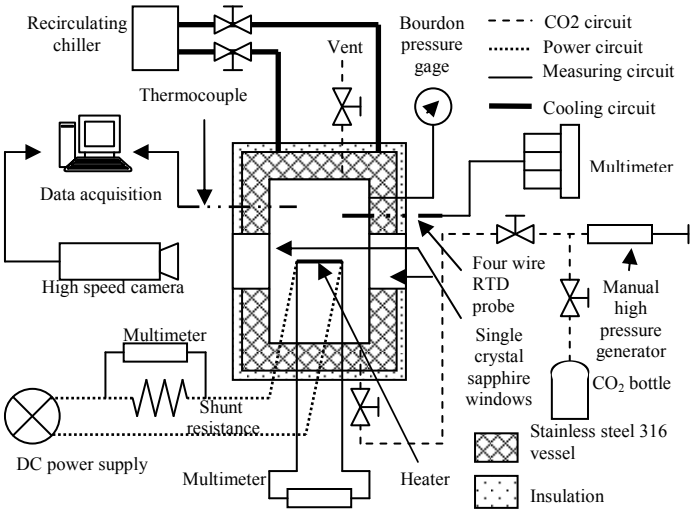

FIGURE 2. SCHEMATIC OF THE EXPERIMENTAL APPARATUS

The bulk fluid temperature is controlled by circulating of a mixture of water and ethylene glycol through channels provided within the vessel's walls. A recirculating chiller is used to control the temperature of the recirculating mixture. The pressure inside the vessel is measured by a bourdon pressure gage, while the temperature of the bulk fluid is measured with a thermocouple and a four-wire RTD probe.

The test fluid used in the experiment is bone dry CO_2. The filling and pressurization of the test chamber is performed using a manual high pressure generator (HiP 62-6-10). Platinum (99.99% pure) was selected as the material for the wires, since its temperature dependant electrical resistance is well known. The resistance of the wire is measured using a four-wire resistance measurement circuit. Two of the wires are used to connect the heater to the DC power supply, while the other two wires are used to measure the voltage drop across the heater wire. This drop is measured using a digital multimeter (Keithley, model: 2100). The current supplied is calculated based on the voltage drop measured across an external shunt resistor. The wire is heated by a constant voltage power source. Fluid properties are calculated using the REFPROP software from NIST [11].

EXPERIMENTAL PROCEDURE

Prior to each test run, the high pressure vessel is filled at room temperature with CO_2. With the cylinder still connected to the test chamber, the vent valve is opened in order to purge the vessel of any impurities. The purging is repeated three times. For the final fill, the temperature of the vessel is lowered to about 8-10 °C. Once the chamber is filled, the pressure in the test chamber is set using the high pressure hand pump. The bulk fluid temperature is set using the external recirculating chiller.

Before each test run, once the bulk conditions are established in the test chamber, the resistance of the heater is measured. This measured resistance and T_b are used as the reference resistance and reference temperature when the heater resistances measured during a test run are converted to temperature. During each test run, T_b and P are maintained constant while the power (and hence T_w) is increased using the DC power supply.

The wire sizes used are 25.4 μm, 76.2 μm and 100 μm for platinum and 101.6 μm for nichrome 60/20. The length of the wires is almost constant, varying from 22.5 mm to 24.2 mm. Table 1 shows the different pressures and bulk temperatures for which experiments were performed.

TABLE 1. EXPERIMENTAL CONDITIONS

platinum, D = 25.4, 76.2 and 100 μm							
P (MPa)	9.60	8.10	7.50	7.34	6.99	6.65	6.30
T_b (°C)	10 25 31 33.3	10 25 31 33.3	10 25 31 33.3	10 20.2 25 30	10 20.2 25 27.8	10 20.2 25	10 20.2

Nichrome 60/20, D = 101.6 μm			
P (MPa)	9.60	8.00	7.50
T_b (°C)	31	31	10 25 31

As shown in Table 1, experiments were conducted at subcritical and supercritical pressures. For the supercritical region, the reduced pressure (P/P_c) varied in the range $1.017 \le P/P_c \le 1.301$, and the reduced bulk temperature ($T_{b,r} = T_b/T_c$) of the fluid varied in the range $0.931 \le T_{b,r} \le 1.008$. For the subcritical region, P/P_c varied in the range $0.855 \le P/P_c \le 0.995$, and $T_{b,r}$ is varied in the range $0.931 \le T_{b,r} \le 0.997$. For each set, T_w is varied from $T_b + 0.1$ °C $\le T_w \le 220$ °C. To investigate the effect of the wire material, a few experiments were conducted using a 101.6 μm diameter nichrome 60/20 wire.

The heat transfer coefficient is calculated as

$$h = \frac{q}{T_w - T_b}, \qquad q = \frac{VI}{A_h} \tag{1}$$

where q is the heat flux, V and I are the voltage and current supplied to the heater, respectively. A_h is the heater surface area ($A_h = \pi Dl$).

UNCERTAINTY ANALYSIS

The accuracy of the bulk temperature measurement is ± 0.1 °C, while the accuracy of the pressure measurement is ± 0.035 MPa. Uncertainty in voltage measurement (voltage drop across the wire and across the shunt resistance) is 0.005 % of full scale reading ± 0.01 mV, and the uncertainty of the shunt resistance is ± 0.5 mΩ.

As a result, the estimated uncertainty in T_w varies from ± 0.2 % to ± 0.03 % as T_w varies from about 10 °C to 220 °C. Uncertainty in the heat flux is almost constant, at ± 1.5 %. Although relative uncertainties in T_w and q are small, for low $T_w - T_b$, the uncertainty in h can be quite large. For example, for $T_w - T_b < 0.3$ °C, uncertainty in h is approximately 100 %. However, the uncertainty in h decreases rapidly to around 5 % when $T_w - T_b > 3$ °C.

It must be noted that even though the uncertainty in P is only ± 0.035 MPa, as P becomes close to P_c, even this small uncertainty in P can result in significant changes in the property values. This is due to the fact that the properties are very sensitive to P, when $P \approx P_c$. This in turn will increase the uncertainty in the calculated dimensionless parameters, such as the Nusselt number (Nu), the Grashof number (Gr) or the Prandtl number (Pr).

EXPERIMENTAL RESULTS AND DISCUSSION

Figure 3 shows the variation of q with T_w for T_b = 10 °C, D = 76.2 μm and for P varying from 6.30 to 9.60 MPa. The log/log scale was chosen so as to display the entire range of data.

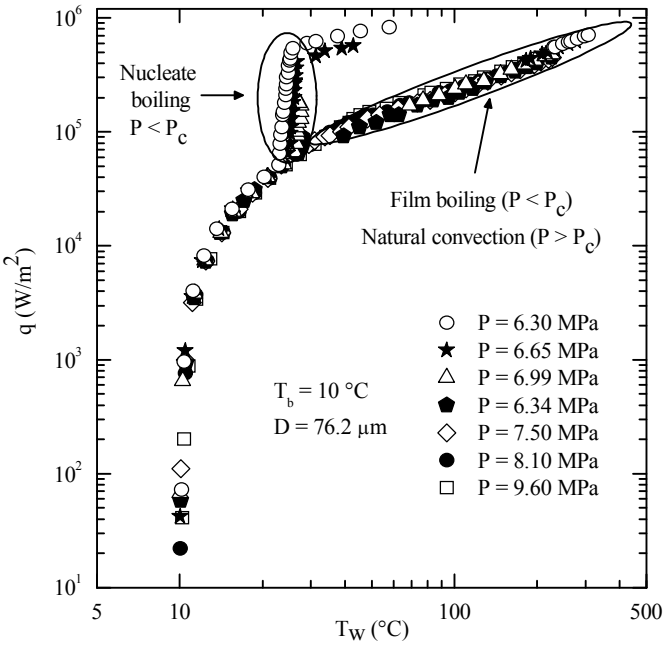

FIGURE 3. VARIATION OF HEAT FLUX WITH WALL TEMPERATURE FOR SUPERCRITICAL AND SUBCRITICAL PRESSURES

The above figure illustrates the similarities between free convection heat transfer at both supercritical and subcritical pressures. Heat flux varies with T_w in a similar way whether $P < P_c$ (before the onset of nucleate boiling) or $P > P_c$. It is also seen in Fig. 3 that the heat transfer phenomenon occurring at $P > P_c$, when $T_w > T_{pc}$, is similar to that observed during film boiling (when $P < P_c$), though no phase change occurs when $P > P_c$. This is because at $P > P_c$, and $T_w > T_{pc}$, the heater surface is completely enveloped in a layer of low-density ("gas-like") fluid. This is similar to heater being enveloped by a vapor film during film boiling.

Figure 4 shows the variation of h with T_w for the same data plotted in Fig. 3. Figures 3 and 4 show that free convection heat transfer pre and post T_{pc} and T_{sat} appear to have similar trends at both

subcritical ($P < P_c$) and supercritical ($P > P_c$) pressures. The differences between subcritical and supercritical pressures became obvious as soon as nucleate boiling begins for subcritical pressures. Boiling heat transfer at near-critical pressures will be the focus of a future study and hence will not be discussed in this paper.

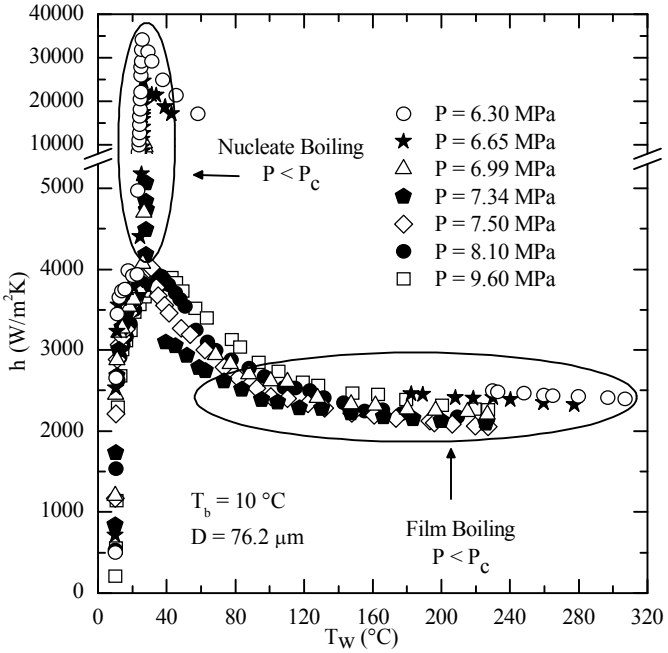

FIGURE 4. VARIATION OF HEAT TRANSFER COEFFICIENT WITH WALL TEMPERATURE FOR SUPERCRITICAL AND SUBCRITICAL PRESSURES

Natural convection heat transfer to subcritical CO_2, $T_w < T_{sat}$

The effect of independent variables on heat transfer coefficient in natural convection is described in a systematic way in this section.

Figure 5 shows the variation of h with (T_w - T_b) for D = 76.2 μm and varying T_b and P; Data for P = 6.65 MPa, T_b = 25 °C; and P = 6.30 MPa are not shown due to limited natural convection data at these conditions. It can be seen in Fig. 5 that, for given $T_w < T_{sat}$, the values of h are larger when T_b is close to the saturation temperature (T_{sat}). Also, the increase in h with (T_w - T_b) is greater for higher T_b. Irrespective of P, at low values of T_w, h increases rapidly with increasing T_w; h increases much more slowly at higher T_w ($T_w - T_b \geq 3$ °C).

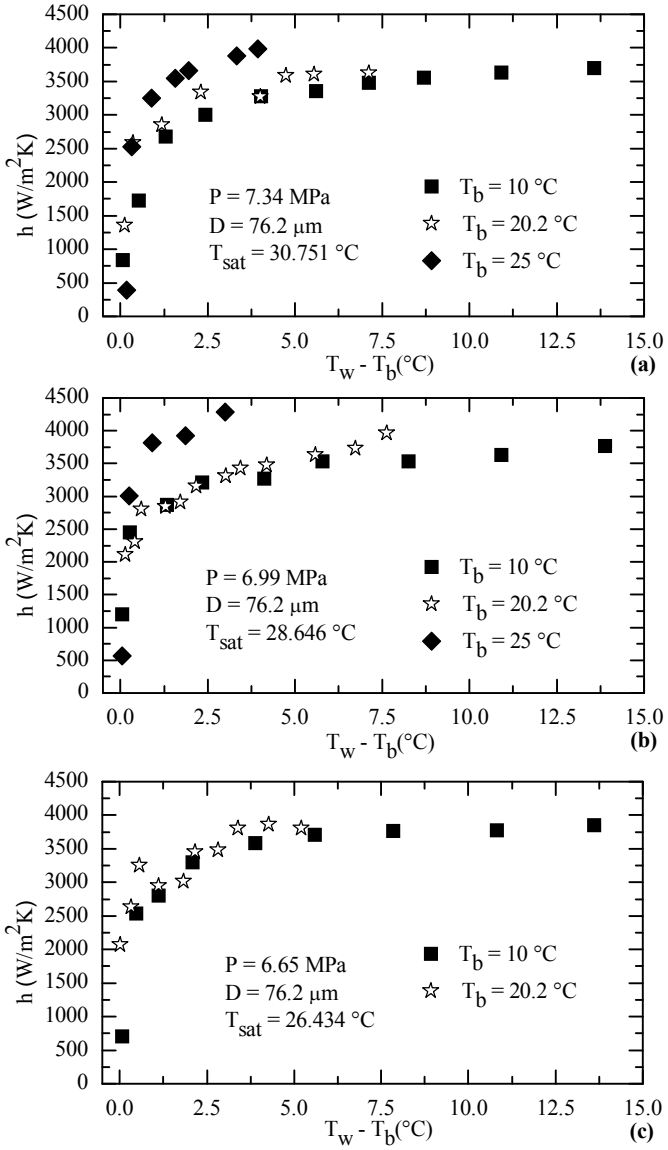

FIGURE 5. VARIATION OF HEAT TRANSFER COEFFICIENT WITH TEMPERATURE DIFFERENCE FOR DIFFERENT BULK TEMPERATURES, AT FIXED PRESSURE

Figure 6 shows the variation of h with ($T_w - T_b$) for D = 76.2 μm for different pressures but at a constant T_b.

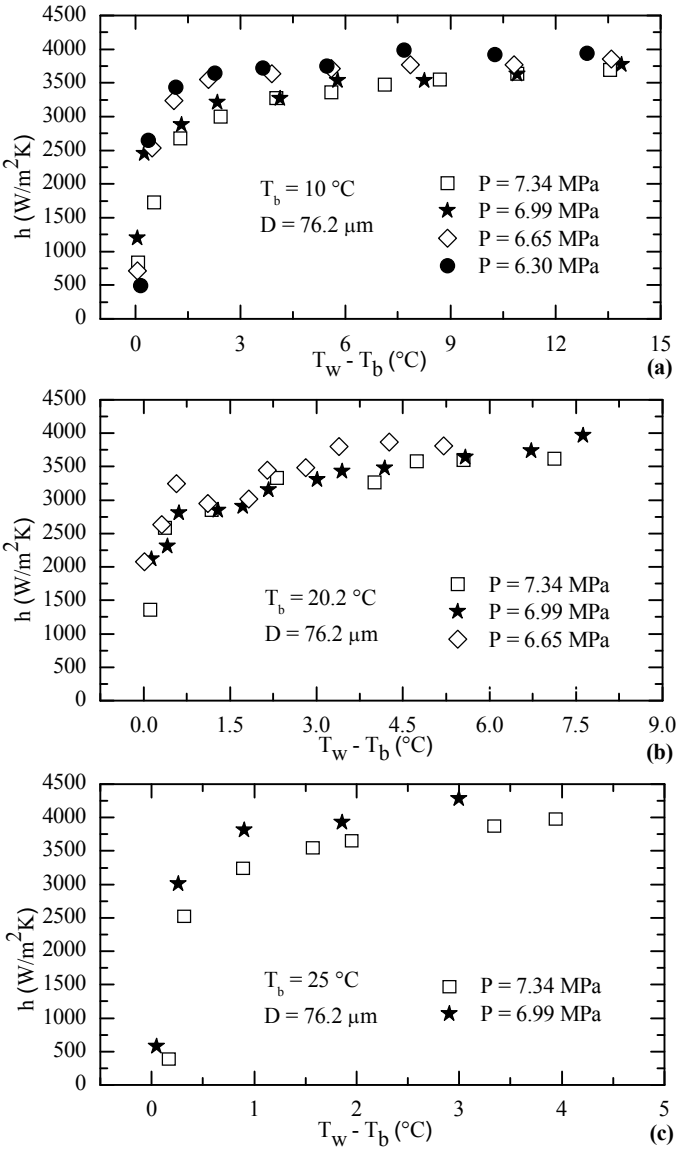

FIGURE 6. VARIATION OF HEAT TRANSFER COEFFICIENT WITH TEMPERATURE DIFFERENCE FOR VARIOUS PRESSURES, AT FIXED BULK TEMPERATURE

From Figs. 6(a)-6(c), it can be seen that for a given T_b, h increases with increasing T_w. Larger values of P yield lower values of h.

The effect of wire diameter is shown in Fig. 7, where h is plotted as a function of T_w - T_b for given T_b and P, for different wire diameters.

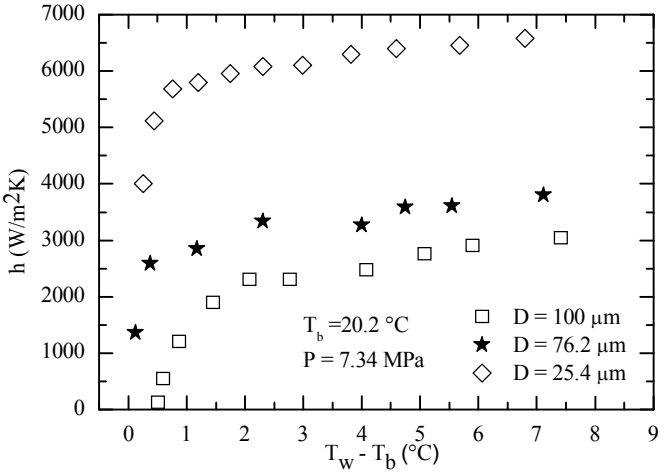

FIGURE 7. VARIATION OF HEAT TRANSFER COEFFICIENT WITH TEMPERATURE DIFFERENCE FOR VARIOUS WIRE DIAMETERS

Wire size appears to have no influence on the general trend of the curves (i.e., the behavior of h with changing T_w). But the difference in wire size appears in the magnitude of h. The magnitude of h, at given P and T_b, is larger as D becomes smaller. The dependence of h on D is found to be $h \propto D^{-0.64}$. Standard textbook correlations [12] give $h \propto D^{-0.25}$ for laminar convection. The dependence of h on D is similar to that reported in [4], where $h \propto D^{-0.625}$.

Natural convection heat transfer to supercritical CO_2

Figure 8 shows the variation of h with T_w for a given D and varying T_b and P. In all cases shown in Fig. 8, h increase rapidly with the increase in T_w (for $T_w < T_{pc}$); reaches a maximum and then decreases with further increase in T_w (for $T_w > T_{pc}$). From Fig. 8(a), it can be seen that the peak value of h increases with T_b provided $T_b < T_{pc}$ (T_{pc} = 31.7 °C). On the other hand, when $T_b > T_{pc}$, h decreases with increasing T_b. Also note that for $T_w < T_{pc}$, the rate of increase in h is strongly dependent on T_b. The closer T_b is to T_{pc}, the greater is the increase in h. The maximum value of h is also higher when T_b is closer to T_{pc}. This is due to the large property variations close to T_{pc}. The heat transfer coefficient shows slight dependence on T_b when T_w is large ($T_w > T_{pc}$). Also note that for all cases, whether $T_b < T_{pc}$ or $T_b > T_{pc}$, when $T_w > T_{pc}$, h is slowly decreasing with the increase in T_w. The transition from $T_w < T_{pc}$ to $T_w > T_{pc}$ is accompanied by a large decrease in the density of the fluid in the immediate vicinity of the heater. When $T_w > T_{pc}$, the heater surface is completely enveloped in a layer of low-density ("gas-like") fluid. While no phase change occurs, this phenomenon is similar to film boiling, when the heater is enveloped by a vapor film.

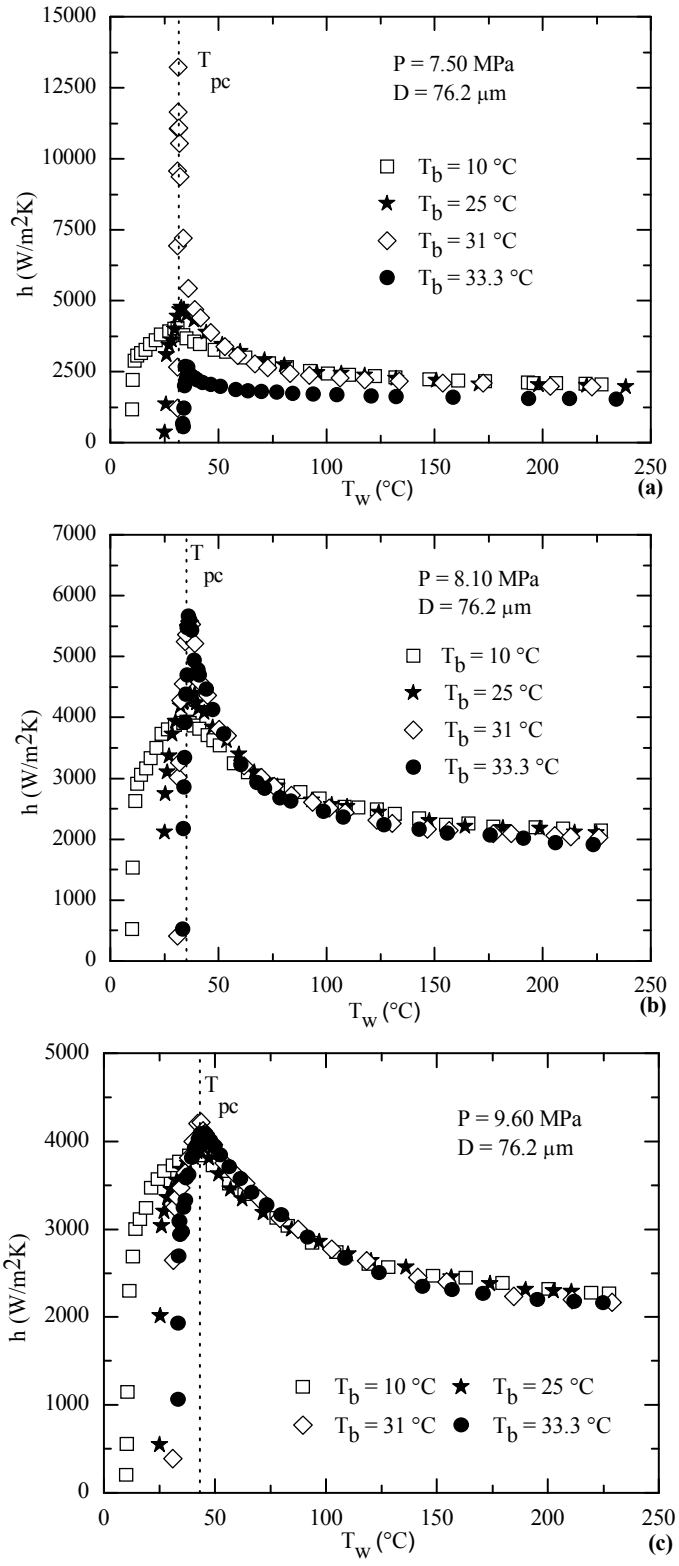

FIGURE 8. VARIATION OF HEAT TRANSFER COEFFICIENT WITH WALL TEMPERATURE FOR DIFFERENT BULK TEMPERATURES, AT A FIXED PRESSURE

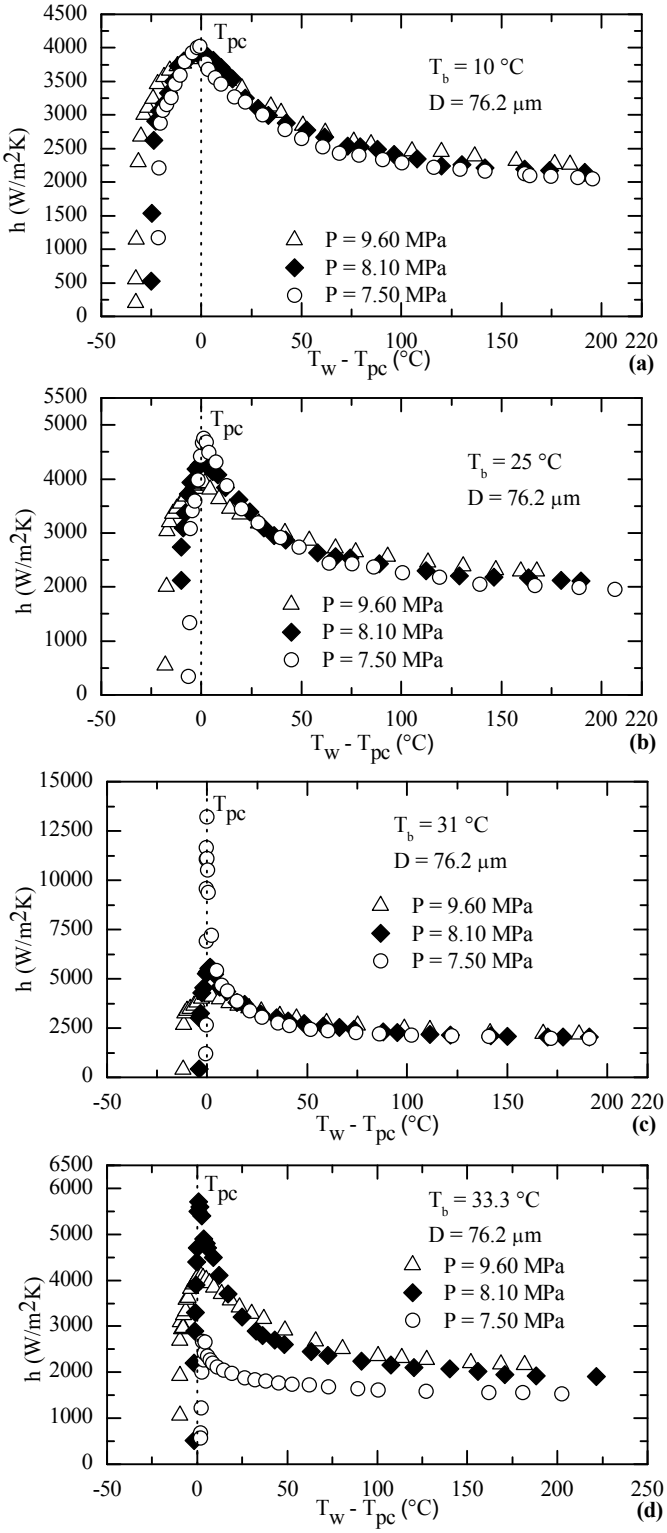

FIGURE 9. VARIATION OF HEAT TRANSFER COEFFICIENT WITH $T_w - T_{pc}$ FOR DIFFERENT PRESSURES, AT FIXED BULK TEMPERATURE

Figures 9 show the variation of h with ($T_w - T_{pc}$) at a fixed T_b when P is varied parametrically. For a given T_b and $T_w < T_{pc}$, h increases with decreasing P. Larger magnitudes of h are obtained as P

becomes close to P_c. For $T_w \approx T_{pc}$, h peaks, and the magnitude of this peak is directly related to P. For $T_w > T_{pc}$, h decreases slightly with the increase in P.

The effects of T_b and P on h are closely related. The influence of P on h is greatest when T_b is close to T_{pc}, as shown in Fig. 9(c). On the other hand, Fig. 9(a) shows that for sufficiently low T_b, the peak values of h are almost independent of P. One can surmise that for a large enough value of P, the effect of T_b would be negligible. Similarly, the influence of T_b on h is greatest when P is close to P_c, as shown in Fig. 9(a, b, c and d).

Fluid properties such as k, c_p and β attain their maximum value at T_{pc}, hence it is reasonable to expect h to be maximum when $T_w = T_{pc}$. While the temperature at which the peak in h occurs is close to T_{pc}, as shown in Fig. 9, it is rarely at T_{pc}. The value of T_w when h is maximum (denoted as $T_{w,peak}$) is always greater than T_{pc}. Figure 10 shows ($T_{w,peak}$ - T_{pc}) as a function of ($T_{pc} - T_b$), for varying T_b and P, and a given D. Experimental results from [9, 13] are included.

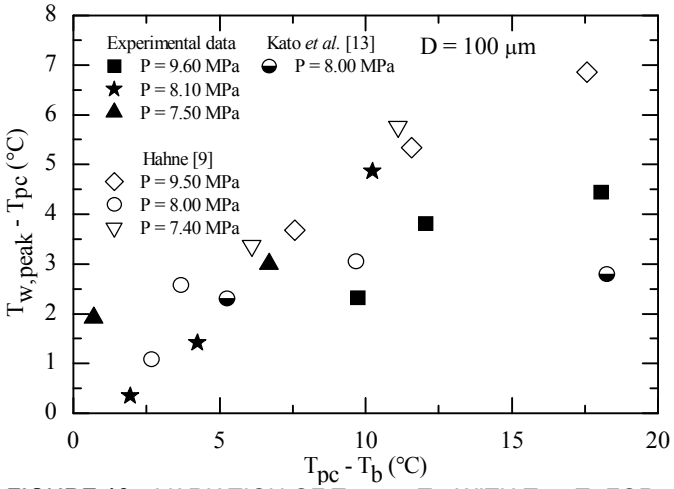

FIGURE 10. VARIATION OF $T_{w,peak}$ - T_{pc} WITH T_{pc} - T_b FOR DIFFERENT PRESSURES AND BULK TEMPERATURES

In spite of the scatter in the data (due to the extreme sensitivity of the peak in h on T_w), a clear trend can be seen in Fig. 10. For a given P, as T_b increases, $T_{w,peak}$ comes closer to T_{pc}. While we could expect $T_{w,peak} = T_{pc}$ for $T_b = T_{pc}$, with the available data it is not possible to estimate the value of T_b for which $T_{w,peak} = T_{pc}$. In addition, it is not possible to discern the reason for this behavior from the experimental data. Detailed numerical simulations are the only way to explain the reason for this.

The effect of wire diameter on natural convection heat transfer to supercritical CO_2 was also studied. Figure 11(a) shows h as a function of T_w for two pressures and various bulk temperatures, for the three platinum wires studied in this work. Wire size appears to have no influence on the general trend of the curves. For the same T_b and P, h increases at the same rate for all wire diameters, it peaks for the same T_w and then decreases at the same rate. This trend is consistent for all data sets, even when $T_b > T_{pc}$. The slight differences between the curves are attributed to the uncertainties, especially in the vicinity of T_{pc}. As can be seen in Fig. 11(a), the wire size affects the values of h. The heat transfer coefficient at given P and T_b increases as D decreases. The dependence of h on D is found to be $h \propto D^{-0.5}$, as shown in Fig. 11(b) for given P and T_b; the dependence is the same for $T_w < T_{pc}$ and $T_w > T_{pc}$. As mentioned earlier, standard textbook correlations [12] give $h \propto D^{-0.25}$ for laminar flow. The present results differ from those obtained by Hahne [9], where $h \propto D^{-0.333}$. Morgan [14], on the other hand, suggests that for $1 \leq Ra \leq 10^4$ (which is the approximate range of this study), $h \propto D^n$, n varying from -0.56 to -0.44. Ghorbani-Tari and Ghajar [15] suggest $h \propto D^{-0.44}$. Kato *et al.* [13] recommend $h \propto D^{-0.25}$, although only one wire size was used in their study. The experimental data for the present study was obtained for 25.4 μm ≤ D ≤ 100 μm. For small wire diameters, the boundary layer surrounding the wire is approximately of the same size as the wire. But for larger diameter, the size of the boundary layer becomes much smaller than the wire diameter. Therefore we could expect the dependence on the diameter to vary with a large increase in wire diameter.

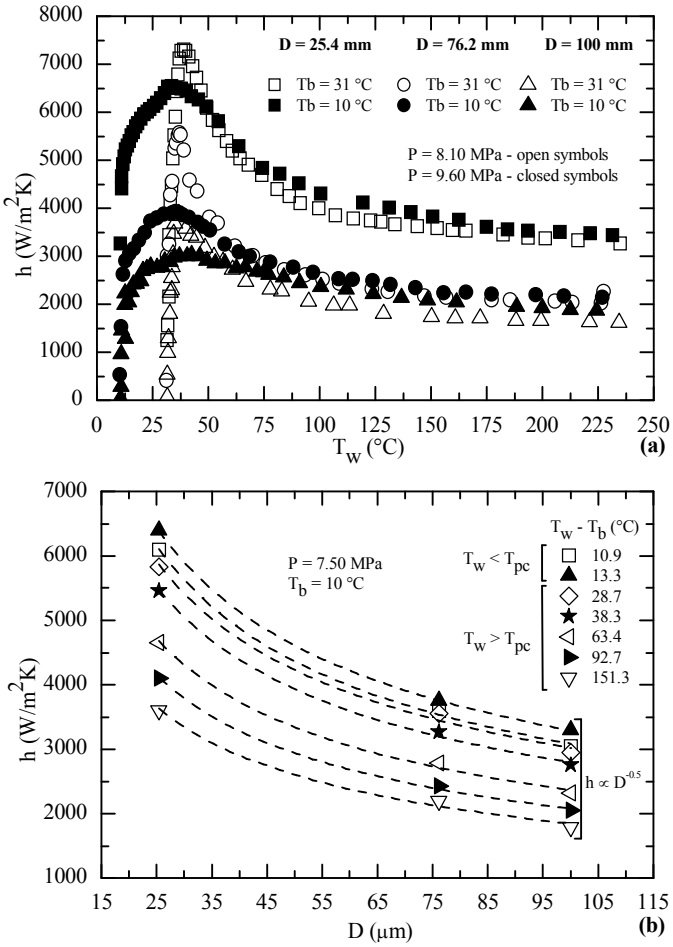

FIGURE 11. (a) VARIATION OF THE HEAT TRANSFER COEFFICIENT WITH THE WALL TEMPERATURE FOR DIFFERENT PRESSURES, BULK TEMPERATURES AND WIRE DIAMETERS - (b) DEPENDANCE OF THE HEAT TRANSFER COEFFICIENT ON THE WIRE DIAMETER FOR VARIOUS T_w - T_b

Visual observations were performed using a high-speed camera. Movies of the convective phenomena were recorded using normal lighting and also using a Schlieren setup. However, since the Schlieren movies did not provide any additional details (when compared to the regular movies), it was not pursued any further.

Visual observations show that thin convective plumes develop when T_b close to T_{pc}, and $T_w > T_{pc}$. Similar observations were reported by Kato *et al.* [13]. Figure 12 shows these plumes emanating from the wire for P = 7.50 MPa, T_b = 31 °C, T_w = 44 °C, q =

$8.15x10^4$ W/m^2, and D = 25.4 μm. Similar flow patterns were observed in [6], [13] and [16].

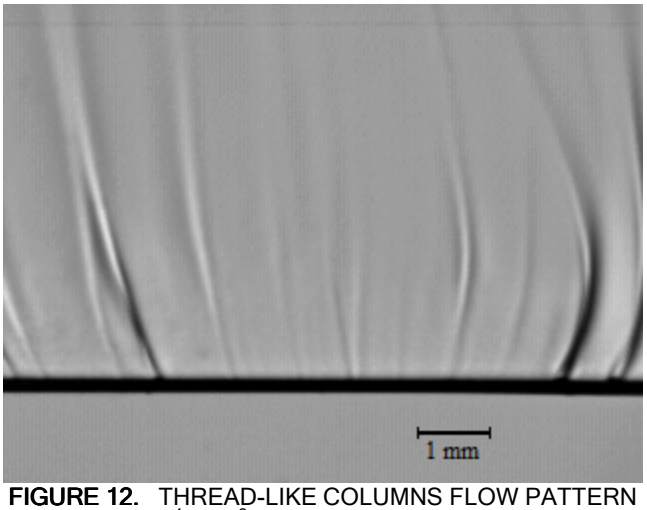

FIGURE 12. THREAD-LIKE COLUMNS FLOW PATTERN FOR q = $8.15x10^4$ W/m^2. P = 7.50 MPa, T_b = 31 °C, T_w = 44 °C AND D = 25.4 μm

Further increase in T_w results in the flow pattern shown in Fig. 13 (T_w = 52 °C and q = $1.10x10^5$ W/m^2).

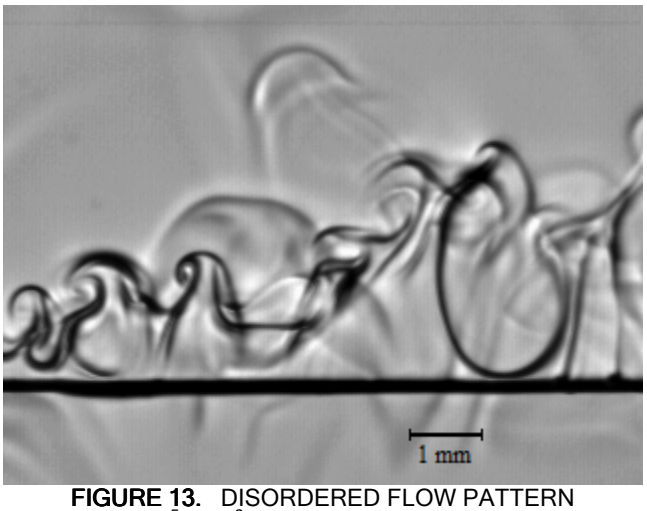

FIGURE 13. DISORDERED FLOW PATTERN FOR q = $1.10x10^5$ W/m^2. P = 7.50 MPa, T_w = 52 °C, T_b = 31 °C, AND D = 25.4 μm

It must be noted that for P close to P_c and for T_b close to T_{pc}, the flow pattern oscillates between thread-like columns (shown in Fig. 12) and structures shown in Fig. 13.

Further increase in T_w results in alternate appearance of orderly thick columns and a disorderly flow pattern, as shown in Fig. 14 for two different time instances (903 ms apart).

The shape of the columns seen in Fig. 14(a) is similar to the ones photographed by Abadzic and Goldstein [6]. If a larger view of the plumes on top of the wire were available, we could expect to see turbulent bursts appear during break up of these columns.

The appearance of these patterns was also reported by Dubrovina and Skripov [16] and Goldstein and Aung [3]. Tamba *et al.* [17] recorded similar flow patterns but for a much higher wall temperature ((T_w - T_b) = 400 °C).

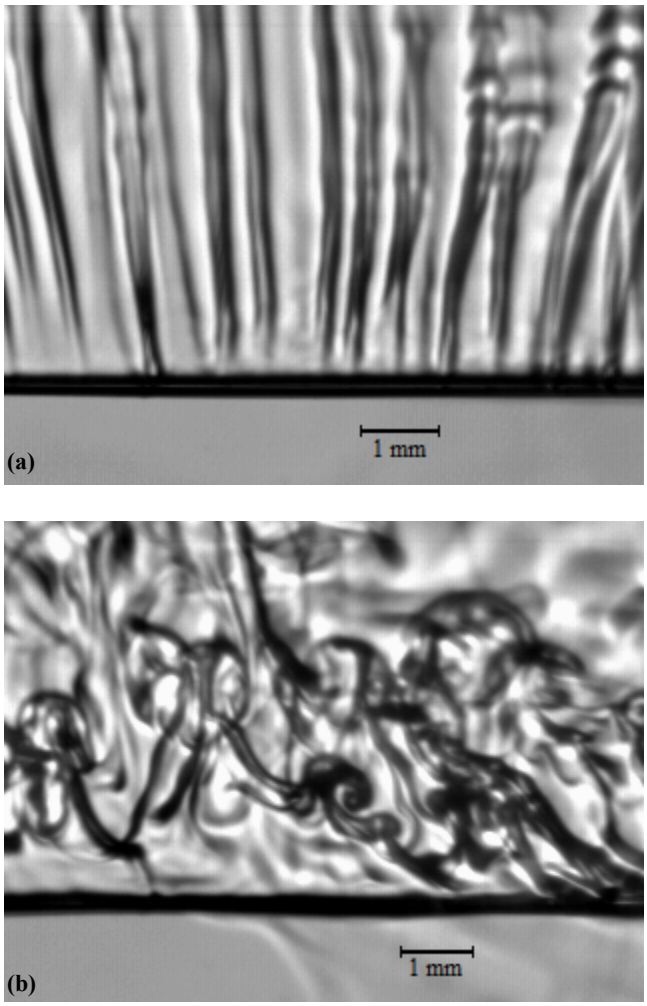

FIGURE 14. (a) THICK COLUMNS FLOW PATTERN, (b) DISORDERED FLOW PATTERN. FOR q = $3.50 .10^5$ W/m^2. P = 7.50 MPa, T_w = 130 °C, T_b = 31 °C, AND D = 25.4 μm

The effect of these patterns was to induce oscillations in the recorded voltage and/or current. This in turn resulted in oscillations in the calculated wire resistance and hence in the calculated wall temperature. Therefore these oscillations associated with shifts in patterns induced a higher uncertainty in the data (though it is difficult to accurately quantify). Also, the intensity of these oscillations appeared to increase with increase in T_w. In the present study, these patterns were only seen for $P \approx P_c$, $T_b \approx T_{pc}$, and $T_w > T_{pc}$.

Goldstein and Aung [3] recorded bubble-like flow patterns using platinum wires, whereas Nishikawa *et al.* [7] and Hahne and Neumann [8] never observed such activity using platinum wires. Observations from [7, 8] are in agreement with the observations of the present study, in that no boiling-like phenomenon occurs at supercritical pressures when platinum wires are used. Knapp and Sabersky [2], and Griffith and Sabersky [5] have described and recorded bubble-like flow patterns. The wire material in [5] was not reported, but [2] used nichrome wires. Nishikawa *et al.* [7] and Hahne and Neumann [8] have compared the flow patterns obtained for different wire materials. In both studies, the use of nichrome wires resulted in the appearance of a boiling-like phenomenon at supercritical pressures. The influence of wire material on h was also investigated in [7, 8]. In [7], results obtained for platinum and alumel

wires were similar, but differences appeared between platinum and nichrome wires were used. The heat transfer coefficient values were found to be larger (by approximately 12 %) using nichrome wires. Differences between platinum and nichrome wires were also reported in [8], h being larger by approximately 10 % with nichrome wires.

To investigate the effect of wire material on heat transfer to supercritical carbon dioxide, a few test runs were performed using a 101.6 μm diameter nichrome 60/20 wire. The flow patterns were recorded. Comparison between heat transfer coefficients obtained with a 100 μm diameter platinum wire (solid symbols) and 101.6 μm diameter nichrome 60/20 (open symbols) are shown in Fig. 15. Figure 15 shows that the results for platinum and nichrome are very similar. The only differences that can be noted are due to uncertainties, especially when $P \approx P_c$. These results disagree with that in [7], where data obtained for platinum and nichrome wires showed significant dependence of h on the wire material.

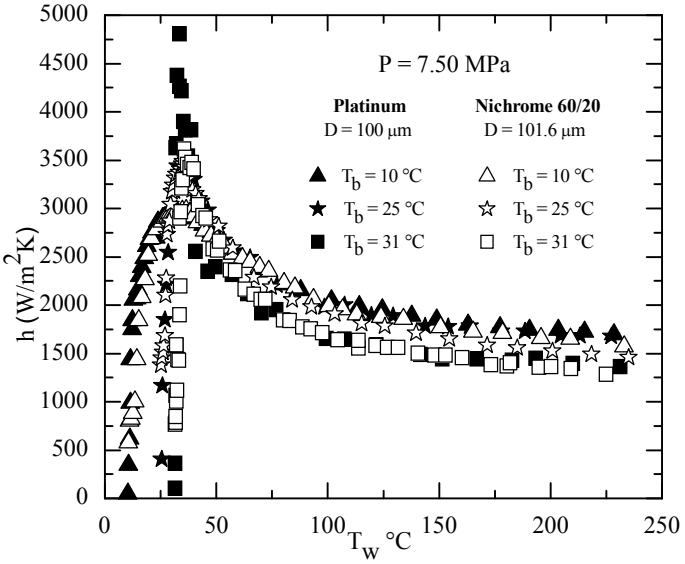

FIGURE 15. INFLUENCE OF THE WIRE MATERIAL ON THE VARIATION OF HEAT TRANSFER COEFFICIENT WITH WALL TEMPERATURE, FOR DIFFERENT PRESSURES, AND BULK TEMPERATURES

Visual observations were performed using a high-speed camera, to investigate the occurrence of the boiling-like phenomena. As shown for platinum (Figs. 12-14), alternating orderly columns and chaotic fluid motion were also observed using a nichrome 60/20 wire, for $P \approx P_c$, $T_b \approx T_{pc}$, and $T_w > T_{pc}$. Figure 16 shows the two flow patterns for nichrome wire for P = 7.50 MPa, T_b = 31 °C, T_w = 72 °C, q = 8.47 .10^4 W/m^2, and D = 101.6 μm.

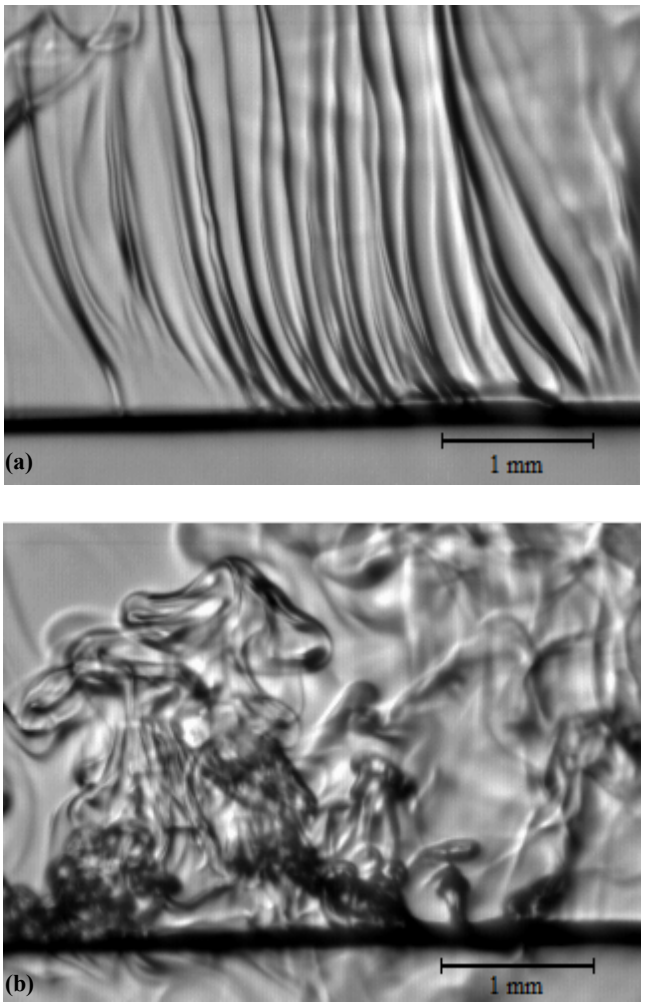

FIGURE 16. (a) THICK COLUMNS FLOW PATTERN, (b) DISORDERED FLOW PATTERN. FOR q = 8.47 .10^4 W/m^2. P = 7.50 MPa, T_w = 72 °C, T_b = 31 °C, AND D = 101.6 μm, Nichrome 60/20

No boiling-like phenomena were observed for 7.50 MPa ≤ P ≤ 9.60 MPa, 10 °C ≤ T_b ≤ 31 °C, even when the exact conditions reported in [8] were reproduced. On certain frames, what could be construed as bubbles were observed during the chaotic flow pattern, as marked in Fig. 17(a) by a dashed line. What could be assumed to be bubbles if one were to just look at a single frame turns out to be nothing more than the formation of chaotic flow structure. Figure 17(b) shows the evolution of these bubble-like structures, 0.25 s after Fig. 17(a) was recorded. It is obvious that these bubble-like structures were in fact just the beginning of chaotic flow patterns.

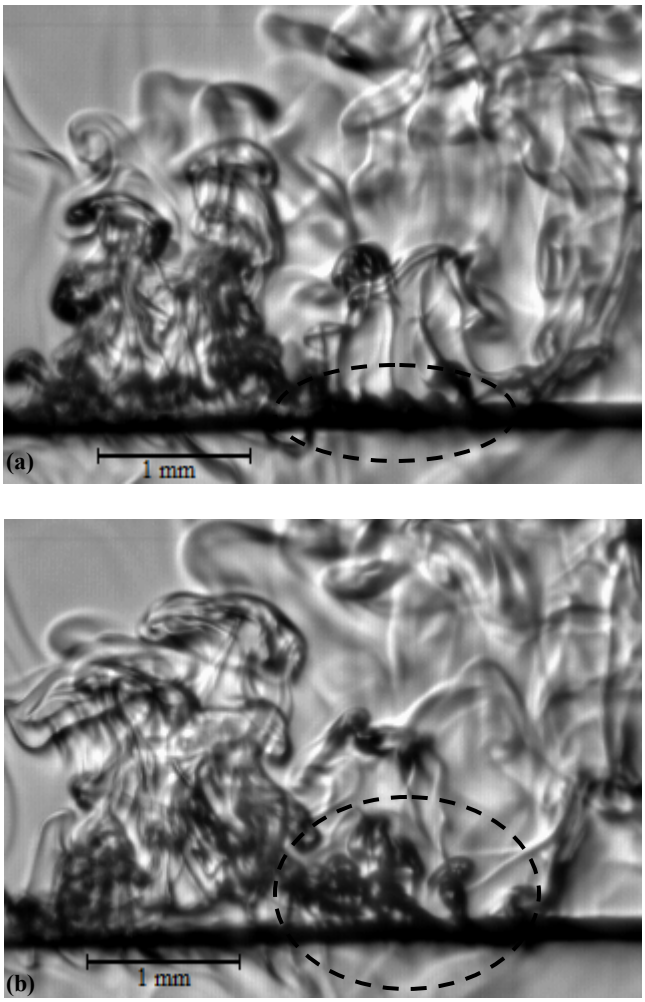

FIGURE 17. BUBBLE-LIKE PATTERN DURING CHAOTIC FLOW PHASE. SAME CONDITIONS AS FOR FIGURE 17. TIME INTERVAL = 0.25 s BETWEEN (a) AND (b)

CORRELATION OF EXPERIMENTAL DATA

Several correlations have been developed for heat transfer to carbon dioxide near critical pressures. The most recent ones, [9, 13, 15], were used to correlate the experimental results obtained in these investigations, but none of them showed a good agreement with the present data. As a consequence, a new correlation had to be developed. But first, the temperature at which fluid properties are to be calculated has to be specified.

Choice of the reference temperature

The behavior of the fluid properties has profound implications on natural convection heat transfer. Additionally, the rapid variation of the properties makes the development of correlations for heat transfer very challenging. The dimensionless natural convection heat transfer (Nu) is usually expressed in the form,

$$\mathrm{Nu} = f(\mathrm{Ra}) \tag{2}$$

where

$$\mathrm{Nu} = \frac{hD}{k},\ \mathrm{Ra} = \mathrm{Gr}.\mathrm{Pr},\ \mathrm{Gr} = \frac{g\beta\left(\frac{\rho_b - \rho_w}{\rho}\right)D^3}{\nu^2},\ \mathrm{Pr} = \frac{\mu c_p}{k} \tag{3}$$

ρ_b is the fluid density at bulk conditions and ρ_w is the fluid density at T_w. ρ is the fluid density at the chosen reference temperature, usually the mean film temperature (T_f), defined as $T_f = (T_w + T_b) / 2$. All the other fluid properties are normally evaluated at T_f.

There are several choices for the reference temperature at which the fluid properties are to be evaluated:

(i) bulk fluid temperature (T_b),
(ii) mean film temperature (T_f),
(iii) wall temperature (T_w).
(iv) integrated mean properties over the range T_b to T_w.

In addition, for natural convection in gases with varying properties, Sparrow and Gregg [18] have suggested the use of the reference temperature, $T_{ref} = T_w - 0.38(T_w - T_b)$. Given all these choices for T_{ref}, it is not obvious which one is to be preferred. No matter which T_{ref} is used, at some point the highly nonlinear behavior of the properties with show up in the correlations.

Kato *et al.* [13] proposed the use of integrated mean property values, defined as,

$$\Phi_i = \frac{1}{T_w - T_b}\int_{T_b}^{T_w} \Phi(T)dT \tag{4}$$

where Φ is the property of interest and the subscript (i) refers to the mean integrated value. However, since c_p and β show singular behavior at T_{pc}, Kato *et al.* [13] proposed approximating c_p as,

$$c_p = \left(\frac{i_w - i_b}{T_w - T_b}\right) \tag{5}$$

where i is the specific enthalpy. Similarly, $\beta\Delta T$ was expressed as,

$$\beta\Delta T = 2\left(\frac{\rho_b - \rho_i}{\rho_i}\right) \tag{6}$$

where ρ_i is the integrated mean value of $\rho(T)$ over the temperature range. Hahne [9] used the same expressions for other properties, only modifying Eq. (5) as,

$$c_p = 2\left(\frac{i_i - i_b}{T_w - T_b}\right) \tag{7}$$

i_i being the integrated mean value of i(T).

The effect of the choice of reference temperatures and the property evaluation methods on Ra and Nu is shown in Fig. 18.

Figures 18(a) and 18(b) show the variation of Nu and Ra respectively as a function of $(T_w - T_b) / T_b$, while Fig. 18(c) shows Nu as a function of Ra. The data plotted in Fig. 18 were obtained in this work for P = 7.50 MPa, T_b = 25 °C and D = 76.2 μm.

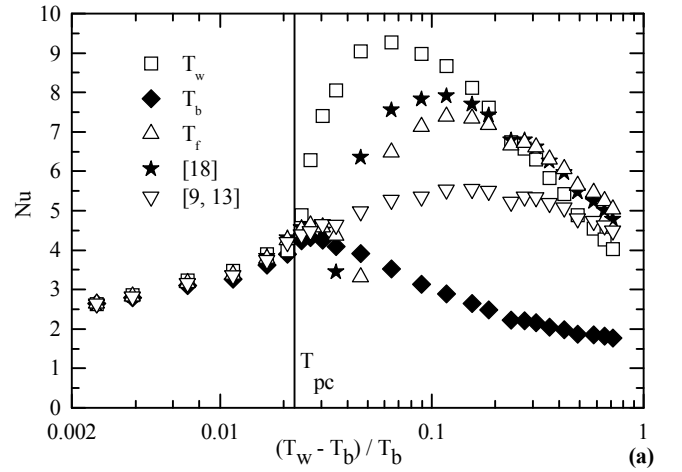

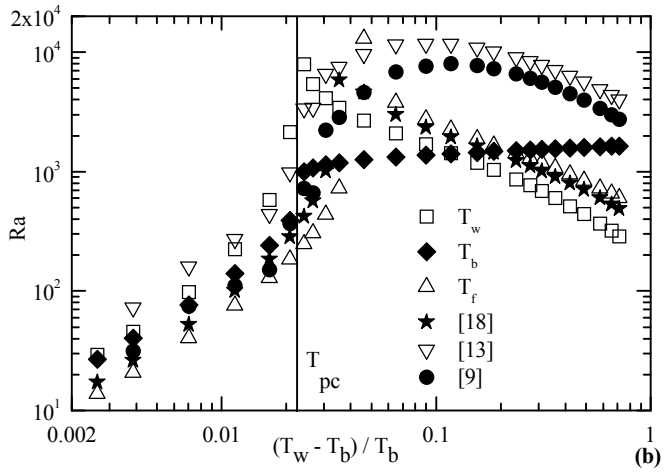

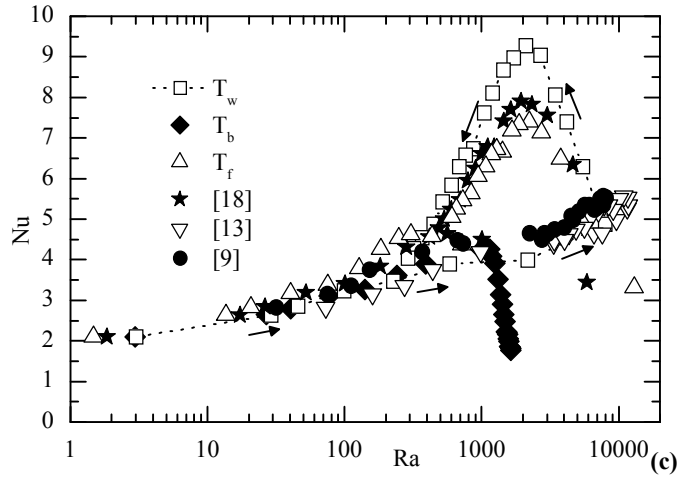

FIGURE 18. (a) NUSSELT NUMBER $(T_w - T_b) / T_b$, (b) RAYLEIGH NUMBER AS A FUNCTION OF $(T_w - T_b) / T_b$ AND (c) NUSSELT NUMBER AS A FUNCTION OF RAYLEIGH NUMBER FOR VARIOUS PROPERTY EVALUATION METHODS

Fig. 18 show that initially, as Ra increases (due to the increase in T_w), Nu increases. When $T_w > T_{pc}$, at a particular temperature both Ra and Nu reach a maximum; further increase in T_w results in the decrease of both Ra and Nu (except when T_b is the reference temperature). The problem that is encountered is the fact that Ra and Nu do not peak at the same value of T_w. Note that there are instances where Ra decreases but Nu continues to increase. This results in the Nu vs. Ra curve looping back upon itself (as shown by a dotted line and arrows in Fig. 18(c), with T_w as the reference temperature). Additionally, the wall temperature at which h and Nu peak do not coincide. This is a direct consequence of the variation of k with T_w. This behavior of Nu and Ra is observed for all reference temperatures (T_w, T_f and T_{ref} suggested in [18]) and property evaluation methods (integrated), except T_b. Using T_b as the reference temperature for property evaluation results in the property values being constant. As a result, both Nu and h increase or decrease in unison, while Ra increases with T_w.

In this study, T_b is used as the reference temperature for property evaluation. Hence, Equs. (2) and (3) become,

$$\mathrm{Nu}_b = f(\mathrm{Ra}_b) \tag{8}$$

with

$$\mathrm{Nu}_b = \frac{hD}{k_b}, \qquad \mathrm{Ra}_b = \mathrm{Gr}_b.\mathrm{Pr}_b,$$
$$\mathrm{Gr}_b = \frac{g\left(\frac{\rho_b - \rho_w}{\rho_b}\right)D^3}{{\nu_b}^2}, \qquad \mathrm{Pr}_b = \frac{\mu_b c_{p,b}}{k_b} \tag{9}$$

While several correlations for free convection heat transfer from a horizontal cylinder have been proposed, the simplest one is the one proposed by McAdams [12]

$$\mathrm{Nu} = C \cdot \mathrm{Ra}^m \tag{10}$$

where C and m are empirical constants and fluid properties are calculated at the mean film temperature. Morgan [14] also chose this simple form for his correlation. Some of the correlations presented for heat transfer to carbon dioxide at supercritical pressures are also based on the same form [13, 15].

In this study we use Eq. (10) as the basis for developing the correlation. The only difference is that all the fluid properties will be calculated at the bulk fluid temperature, for the reasons discussed earlier.

Correlation of the experimental data is done in two parts; one for subcritical pressures ($P < P_c$) and one for supercritical pressures ($P > P_c$). The supercritical part is further subdivided into two; one for $T_w < T_{pc}$ and another for $T_w > T_{pc}$. This is due to the fact that h increased with T_w for $T_w < T_{pc}$ and decreased with T_w when $T_w > T_{pc}$. Consequently, the exponent in Eq. (10) is positive for the first part and negative for the second. No correlation was developed for $T_b > T_{pc}$, since experiments were conducted for only one pressure and one bulk temperature.

Correlation for $P < P_c$

Correlation of natural convection data was complicated by the larger uncertainties in the narrow range of temperatures in which natural convection exists, the data obtained for different pressures and bulk fluid temperature is correlated as,

$$Nu_b = 0.95 Ra_b^{0.12} \left(\frac{i_c}{i_{sat} - i_b} \right)^{0.3} \quad (11)$$

with $8.1 \times 10^{-2} \le Ra_b \le 6.2 \times 10^2$.

In Eq. (11) the term $(i_c / (i_{sat} - i_b))^{0.3}$ accounts for the effects of varying T_b and P on the thermophysical properties, with i_c being the enthalpy of CO_2 at critical conditions (P_c and T_c). The Rayleigh number (Ra_b) is defined as in Eq. (9). Note that the denominator of the term $(i_c / (i_{sat} - i_b))^{0.3}$ will go to zero when $T_b = T_{sat}$, and so Eq. (11) can only be used for $T_b < T_{sat}$.

It should be noted that Grigull and Abadzic [4] proposed a correlation for free convection heat transfer at subcritical pressures of the form

$$Nu = 0.94 Ra^{0.125} \quad (12)$$

with properties calculated at the mean film temperature.

Figure 19 shows comparison of the experimental data with the predictions of heat transfer coefficient from the present correlation (Eq. (11)) and the one given in [4] (Eq. (12)). Note that in Fig. 19 we plot h instead of Nu, because Eq. (11) and Eq. (12) do not use the same property evaluation method. The predictions from the present correlation (Eq. (11)) match well with the experimental data, but the predictions from the correlation given in [4] systematically underpredict the values of h.

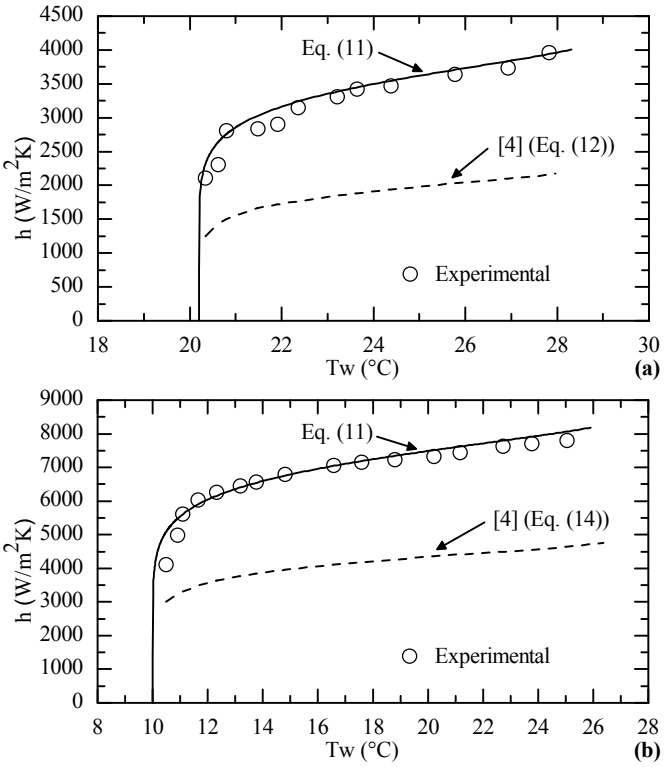

FIGURE 19. COMPARISON BETWEEN EXPERIMENTAL AND PREDICTED VALUES OF THE HEAT TRANSFER COEFFICIENT FOR VARIOUS EXPERIMENTAL CONDITIONS: (a) P = 6.99 MPa, T_b = 20.2 °C, D = 76.2 μm, (b) P = 6.65 MPa, T_b = 10 °C, D = 25.4 μm

The comparison between predicted (Eq. (11)) and experimental Nu is shown in Fig. 20. The predicted values are in agreement with the experimental results within ± 15 %.

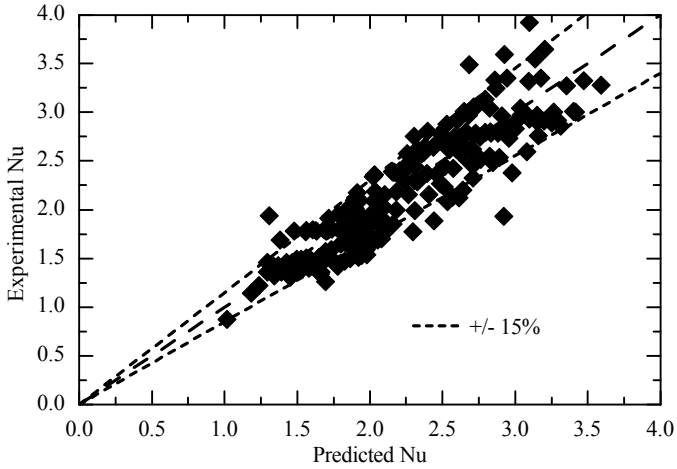

FIGURE 20. COMPARISON BETWEEN EXPERIMENTAL AND PREDICTED VALUES OF THE NUSSELT NUMBER FOR $T_w < T_s$, $T_b < T_s$ AT SUBCRITICAL PRESSURES. WIRE DIAMETERS RANGE FROM 25.4 μm to 100 μm. RAYLEIGH NUMBER AT BULK CONDITIONS (Eq. (9)) RANGE FROM 300 TO 1.5×10^7

Correlation for $P > P_c$, $T_w < T_{pc}$

Equation (11) was modified slightly to correlate the data for $P > P_c$ and $T_w < T_{pc}$. Note that for $P > P_c$, T_{pc} replaces T_{sat} and hence i_{pc} replaces i_{sat} in Eq. (11). Additionally, since h was found to be proportional to $D^{-0.5}$ (as compared to $h \propto D^{-0.64}$ for $P < P_c$), the term $Ga_c^{0.047}$ is used to account for the diameter effect. The Galileo Number (Ga) is defined as,

$$Ga = \frac{gD^3}{\nu^2} \quad (13)$$

and all properties are evaluated at critical conditions (P_c and T_c). The modified version of Eq. (11) is given as,

$$Nu_b = 1.34 Ra_b^{0.12} \left(\frac{i_c}{i_{pc} - i_b} \right)^{0.3} Ga_c^{0.047} \quad (14)$$

with $1 \le Ra_b \le 3.6 \times 10^5$. Ra is defined as in Eq. (9).

Correlation for $P > P_c$, $T_w > T_{pc}$

For $T_w > T_{pc}$, Gr defined based on $\beta\Delta T$ was used instead of $(\Delta\rho/\rho)$. For all the experimental data, the dependence of Nu on $\Delta\rho/\rho$, therefore on Ra as in Eq. (3), was found to be constant for $T_w < T_{pc}$ and for $P < P_c$. But, as shown in Fig. 21, this is not true for $T_w > T_{pc}$. For $T_w > T_{pc}$, Nu was found to be proportional to $\beta\Delta T$, thus to Ra defined with $\beta\Delta T$ and not $\Delta\rho/\rho$.

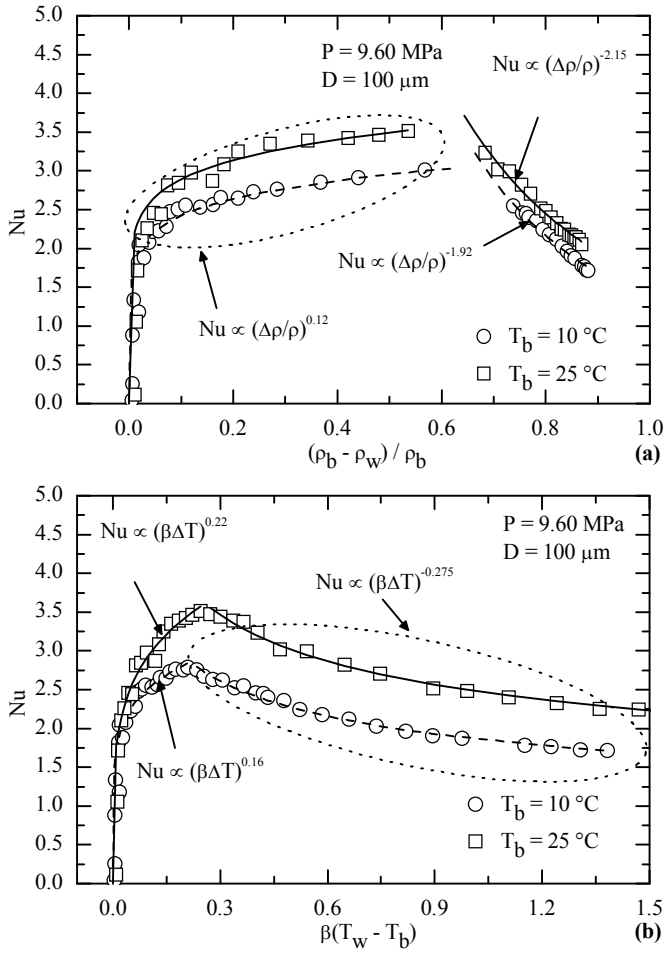

FIGURE 21. Nu AS A FUNCTION OF (a) $\beta(T_w - T_b)$ AND (b) $(\rho_w - \rho_b) / \rho_b$

The fact that the properties are calculated at T_b might be a reason for this phenomenon. The final correlation can be expressed as,

$$Nu_b = 0.208 Ra_b^{-0.275} \left(\frac{i_c}{i_{pc} - i_b} \right) Ga_c^{0.44} \qquad (15)$$

Note that for both Eq. (14) and Eq. (15), $i_{pc} - i_b$ will go to zero when $T_b = T_{pc}$, and so cannot be used for $T_b = T_{pc}$.

Figure 22 shows comparisons of the experimental data with the predictions from the correlations (Eq. (14) and Eq. (15)) for various conditions.

The predictions match well with the experimental data. Note that the maximum value of h is at the intersection of the two curves (Eq. (14) and Eq. (15)). It is important to note that the correlations show the same trend as the experimental data. For example, for given P and D, as T_b increases, the maximum value of h increases.

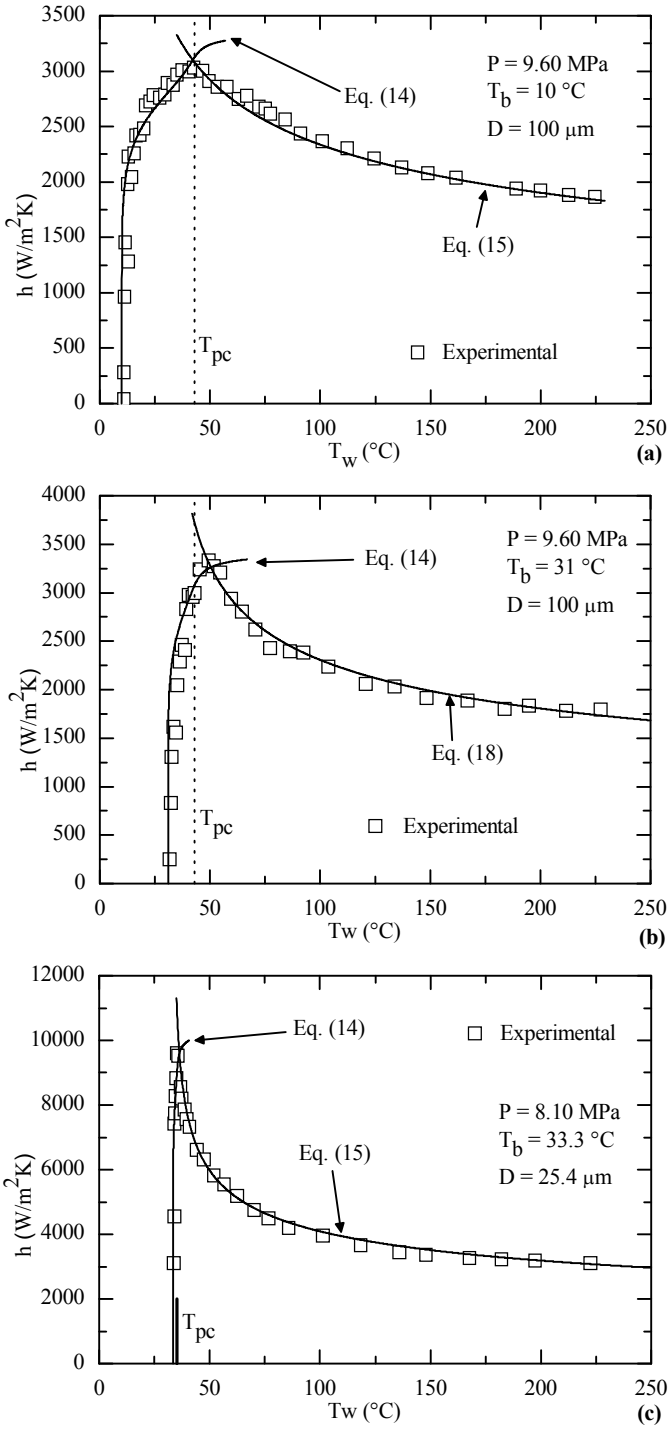

FIGURE 22. COMPARISON BETWEEN EXPERIMENTAL AND PREDICTED VALUES OF THE HEAT TRANSFER COEFFICIENT FOR VARIOUS EXPERIMENTAL CONDITIONS

Figure 23 shows the comparison between the experimental data and the correlations available in the literature [9, 13, and 15], for the same conditions as in Fig. 22.

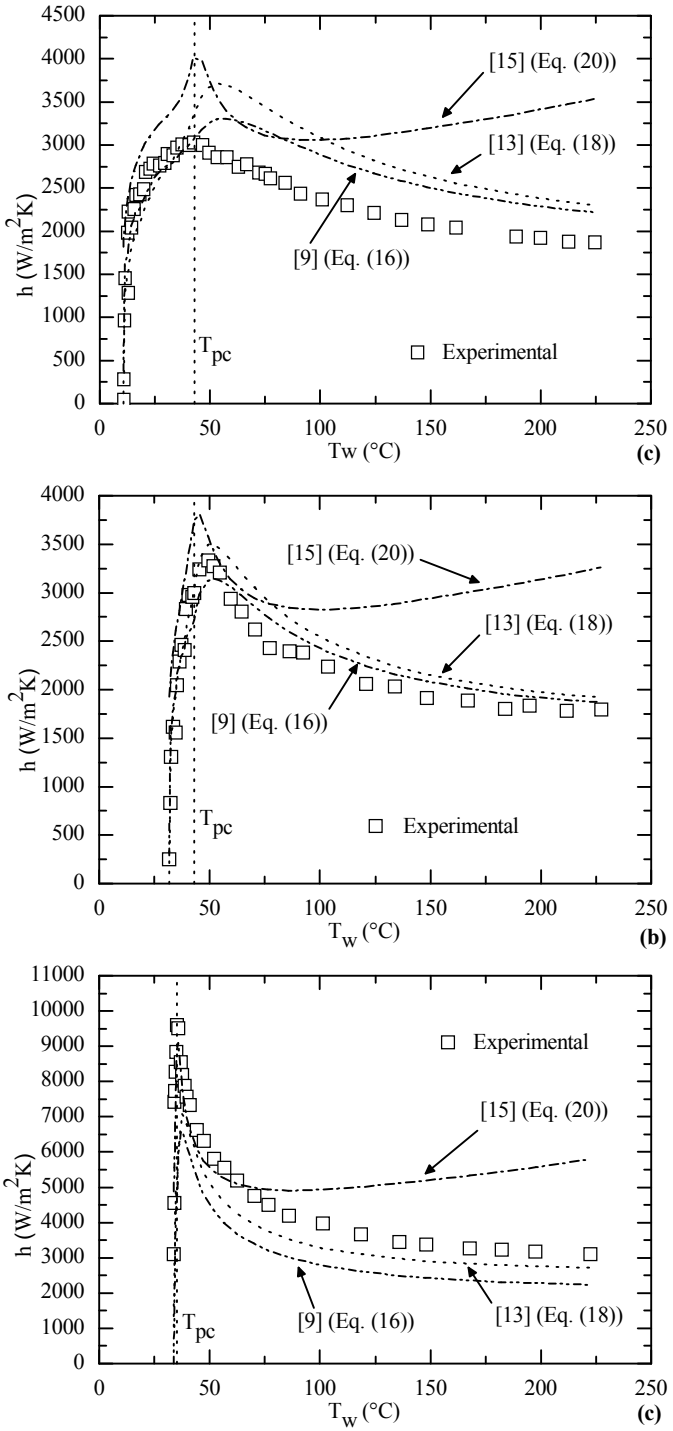

FIGURE 23. COMPARISON BETWEEN EXPERIMENTAL AND PREDICTED VALUES OF THE HEAT TRANSFER COEFFICIENT FOR VARIOUS EXPERIMENTAL CONDITIONS

For the sake of completeness, the correlations available in the literature are given below:

Hahne [9]:

$$\mathrm{Nu_i} = \left(0.35 + 0.25\mathrm{Ra_i}^{1/8} + 0.45\mathrm{Ra_i}^{1/4}\right)\left(1 + f_1 f_2 f_3\right)^{-1} \quad (16)$$

where

$$\mathrm{Ra_i} = \mathrm{Gr_i}\mathrm{Pr_i}, \quad \mathrm{Gr_i} = \frac{2g\left(\frac{\rho_b - \rho_i}{\rho_i}\right)D^3}{\nu_i^{\,2}}, \quad \mathrm{Pr_i} = \frac{2\mu_i\left(\frac{i_i - i_b}{T_w - T_b}\right)}{k_i}$$

$$f_1 = x\mathrm{e}^{-x}, \quad x = 4.5\sqrt{\frac{T_w - T_{pc}}{T_c}}, \quad (17)$$

$$f_2 = \tanh\left(30\frac{T_{pc} - T_b}{T_c}\right),$$

$$f_3 = 1 - 0.3\tanh\left(15\frac{P - P_c}{P_c}\right)$$

for 10 °C ≤ T_w ≤ 600 °C, 10 °C ≤ T_b ≤ 50 °C, 7.40 MPa ≤ P ≤ 9.00 MPa and 50 μm ≤ D ≤ 300 μm.

.

Kato *et al.* [13]:

$$\mathrm{Nu_i} = 0.53\mathrm{Ra_i}^{1/4} \quad (18)$$

where

$$\mathrm{Ra_i} = \mathrm{Gr_i}\mathrm{Pr_i}, \quad \mathrm{Gr_i} = \frac{2g\left(\frac{\rho_b - \rho_i}{\rho_i}\right)D^3}{\nu_i^{\,2}}, \quad \mathrm{Pr_i} = \frac{\mu_i\left(\frac{i_w - i_b}{T_w - T_b}\right)}{k_i} \quad (19)$$

for 15.1 °C ≤ T_w ≤ 55 °C, 15.1 °C ≤ T_b ≤ 46.2 °C, 8.00 MPa ≤ P ≤ 10.00 MPa and D = 200 μm.

Dimensionless numbers in the above correlations are based on integrated thermophysical properties.

Ghorbani-Tari and Ghajar [15]:

$$\mathrm{Nu_b} = 1.153\mathrm{Ra_b}^{0.187}\left(\frac{\rho_w}{\rho_b}\right)^{0.045}\left(\frac{\overline{C_p}}{C_{p,b}}\right)^{0.132}\left(\frac{k_w}{k_b}\right)^{0.722}\left(\frac{\mu_w}{\mu_b}\right)^{-0.110} \quad (20)$$

where

$$\mathrm{Ra_b} = \mathrm{Gr_b}\mathrm{Pr_b}, \ \mathrm{Gr_b} = \frac{g\left(\frac{\rho_b - \rho_w}{\rho_w}\right)D^3}{\nu_b^{\,2}}, \ \mathrm{Pr_b} = \frac{\mu_b C_{p,b}}{k_b}, \ \overline{C_p} = \left(\frac{i_w - i_b}{T_w - T_b}\right) \quad (21)$$

for 8.82 x 10^1 < $\mathrm{Ra_b}$ < 1.02 x 10^4, 10 °C ≤ T_w ≤ 200 °C, 10 °C ≤ T_b ≤ 55 °C, 7.40 MPa ≤ P ≤ 9.52 MPa and D = 100 μm. This correlation is based on data that had been reported in the literature.

Note that in the above correlations the effect of cylinder diameter is accounted for in Ra, and that only [9] obtained data for several cylinder diameters.

Refering to the comparison shown in Fig. 23, it is clear that Eq. (20) [15] does a poor job of predicting the experimental data, especially at large values of T_w, even for the same wire diameter as used for the development of the correlation. Equations (16) [9] and (18) [13] predict the same trend as the present experimental data, though the predicted values differ somewhat from the experimental data. Also note that the diameter effect is not accounted for correctly. The predicted values overpredict the experimental data for D =100 μm (Figs. 23(a) and 23(b)). On the other hand, they underpredict the experimental data for D = 25.4 μm (Fig. 23(c)).

Figure 24(a) shows the comparison between predictions (from Eq. (14)) and data for Nu, for $T_w < T_{pc}$ and $T_b < T_{pc}$. The data presented include data from Hahne [9] and Nishikawa *et al.* [7]. The range of parameters is:

- 25.4 μm ≤ D ≤ 300 μm,
- 7.40 MPa ≤ P ≤ 9.60 MPa,
- 10 °C ≤ T_b ≤ 33.3 °C,
- 1 ≤ Ra_b ≤ 3.6 x 10^5,
- T_w up to 530 °C.

Data from the present study, along with data from Hahne [9], Goldstein and Aung [3], Abadzic and Goldstein [6], Tamba *et al.* [17] and Nishikawa *et al.* [7] was compiled for $T_w > T_{pc}$ and $T_b < T_{pc}$. Comparison between predicted (from Eq. (15)) and experimental Nusselt Numbers is presented in Fig. 24(b). The range of parameters is:

- 25.4 μm ≤ D ≤ 381 μm,
- 7.40 MPa ≤ P ≤ 9.60 MPa,
- 10 °C ≤ T_b ≤ 33.3 °C,
- 300 ≤ Ra_b ≤ 1.5 x 10^7,
- T_w up to 970 °C.

The comparison shows that the correlation predicts almost all of the data within ± 15 %. Only exception being the data from [7]. Comparison between experimental results from [7] and with experimental data from [9] and [3] for $T_w > T_{pc}$, shows large differences for the same experimental conditions. This could explain the deviation between experimental values of Nu from [7] and predicted values. Data points predicted outside the ± 15 % range, from the present study and [9], are for experimental conditions very close to critical pressure and temperature, i.e., 7.40 MPa ≤ P ≤ 7.50 MPa and 30 °C ≤ T_b ≤ 31 °C. The extreme temperature dependence of the fluid properties as well as the larger uncertainties in data in this region could be the reason for the observed discrepancy.

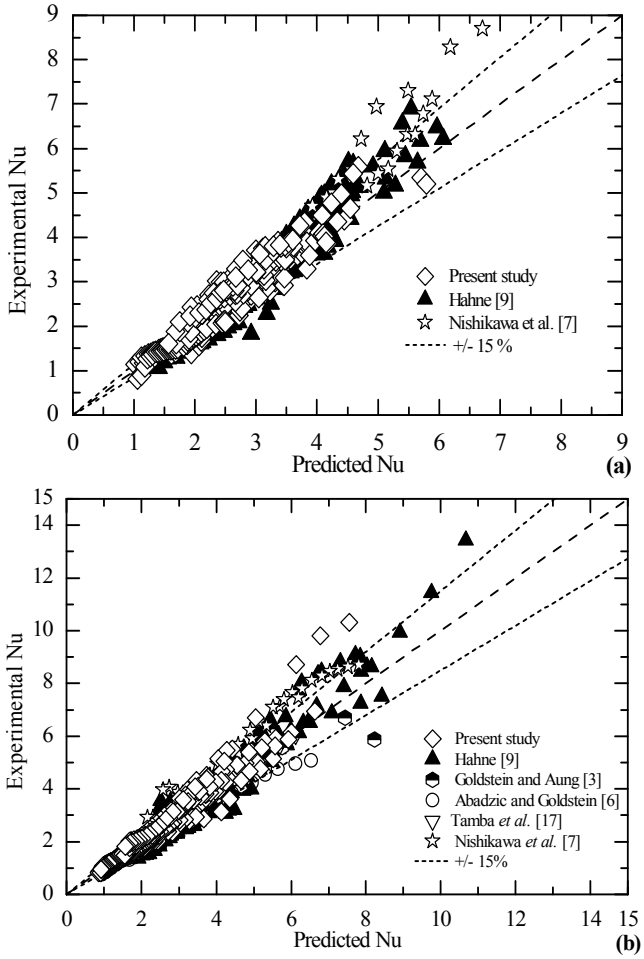

FIGURE 24. COMPARISON BETWEEN EXPERIMENTAL AND PREDICTED VALUES OF Nu.
(a) $T_w < T_{pc}$, $T_b < T_{pc}$, $P > P_c$. (b) $T_w > T_{pc}$, $T_b < T_{pc}$, $P > P_c$

To extend the range of the present correlations (Eq. (14) and Eq. (15)), the predicted values were compared with the experimental data of [13] and [19]. The data in [13] were for D = 2 mm while those in [19] were obtained using 3, 6 and 9 mm diameter cylinders. Hollow tubes made of stainless steel were used in both studies. The values predicted (using Eqs. (14) and (15)) were found to be much lower (2-3 times lower) than the experimental data from [13, 19]. The reason for this difference appears to be the dependence of h on D changes as D increases (i.e. the film thickness becomes much less than D as D becomes large).

CONCLUSIONS

Experiments on natural convection heat transfer from small wires to CO_2 at near-critical pressures have been performed. Experimental results highlight the extreme dependence of h on several parameters, namely: (1) pressure, (2) bulk fluid temperature, (3) wire temperature and (4) wire diameter. Based on the analysis of the obtained data, correlations have been developed to predict Nu at various conditions. These conditions are the following,

(1) Subcritical pressures ($P < P_c$) and $T_w < T_s$: Eq. (11),
(2) Supercritical pressures ($P > P_c$) and $T_w < T_{pc}$: Eq. (14),
(3) Supercritical pressures ($P > P_c$) and $T_w > T_{pc}$: Eq. (15).

The correlations developed predict almost all the experimental data from the current study and those obtained from the literature to within ± 15 %. Visual observations during experiments showed no boiling-like activity for both platinum and nichrome 60/20 wires. Only thread-like column and chaotic flow patterns were observed.

ACKNOWLEDGEMENTS

This study was supported by the National Science Foundation under grant # CTS-0553571.

REFERENCES

[1] Pioro, I. L., Khartabil, H. F., Duffey, R. B., 2004, "Heat Transfer to Supercritical Fluids Flowing in Channels - Empirical Correlations (survey)," *Nuclear Engineering and Design*, vol. 230, pp. 69–91.

[2] Knapp, K. K., and Sabersky, R. H., 1966, "Free Convection Heat Transfer to Carbon Dioxide near the Critical Point," *International Journal of Heat and Mass Transfer*, vol. 9, pp. 41-51.

[3] Goldstein, R. J., and Aung, W., 1968, "Heat Transfer by Free Convection from a Horizontal Wire to Carbon Dioxide in the Critical Region" Transactions of the American Society of Mechanical Engineers, *Journal of Heat Transfer*, vol. 90, part 2, pp. 51-55.

[4] Grigull, U., and Abadzic, E., 1967-68, "Heat Transfer from a Wire in the Critical Region," Proceedings of the Institution of Mechanical Engineers, vol. 182, part 3 I, paper 8, pp. 52-57.

[5] Griffith, J. D., and Sabersky, R. H., 1960, "Convection in a Fluid at Supercritical Pressures," *Journal of the American Rocket Society*, vol. 30, number 3, pp.289-291.

[6] Abadzic, E., and Goldstein, R. J., 1970, "Film Boiling and Free Convection Heat Transfer to Carbon Dioxide near the Critical State," *International Journal of Heat and Mass Transfer*, vol. 13, pp. 1163-1175.

[7] Nishikawa, K., Ito, T., and Yamashita, H., 1973, "Free-Convective Heat Transfer to a Supercritical Fluid," Transactions of the American Society of Mechanical Engineers, *Journal of Heat Transfer*, vol. 95, part 2, pp. 187-191.

[8] Hahne, E. W. P., and Neumann, R. J., 1981, "Boiling-like Phenomena Free-Convection Heat Transfer at Supercritical Pressures," *Wärme- und Stoffübertragung*, vol. 15, pp. 171-180.

[9] Hahne, E. W. P., 1985, "Natural Convection in the Near Critical Region and Its Application in Heat Pipes," in *Natural Convection: Fundamentals and Applications*, NATO ASI Book, edited by Kakaç, S., Aung, W., and Viskanta, R., Hemisphere Publishing Corporation, Washington.

[10] Warrier, G. R., Rousselet, Y., and Dhir, V., K., 2011, "A Numerical Investigation of Heat Transfer from Small Horizontal Cylinders at Near-Critical Pressures" ASME/JSME 8th Thermal Engineering Joint Conference, AJTEC2011-44494.

[11] REFPROP, Reference Fluid Thermodynamic and transport Properties, NIST Standard Reference Database 23, version 8.0.

[12] McAdams, W. H., 1954, *Heat Transmission*, 3rd Edition, McGraw-Hill, New York.

[13] Kato, H., Nishiwaki, N., and Hirata, M., 1968, "Studies on the Heat Transfer of Fluids at a Supercritical Pressure," *Bulletin of the Japan Society of Mechanical Engineers*, vol. 11, pp. 654-663.

[14] Morgan, V. T., 1975, "Heat Transfer from Cylinders," *Advances in Heat Transfer*, vol. 11, pp. 199-264.

[15] Ghorbani-Tari, S., and Ghajar, A. J., 1985, "Improved Free Convective Heat Transfer Correlations in the Near-Critical Region," *American Institute of Aeronautics and Astronautics Journal*, vol. 23, pp. 1647-1649.

[16] Dubrovina, E. N., and Skripov, V. P., 1965, "Convection and Heat Transfer near the Critical Point of Carbon Dioxide," *Zhurnal Prikladnoi Mekhaniki i Tekhnicheskoi Fiziki*, vol. 1, pp. 115-119.

[17] Tamba, J., Takahashi, T., Ohara, T., Aihara, T., 1998, "Transition from Boiling to Free Convection in Supercritical Fluid," *Experimental Thermal and Fluid Science*, vol. 17, pp. 248-255.

[18] Sparrow, E. M., and Gregg, J. L., 1958, "The variable fluid-property problem in free convection," Transactions of the American Society of Mechanical Engineers, *Journal of Heat Transfer*, vol. 80, pp. 879-886.

[19] Beschastnov, S., P., and Petrov, V., P., 1973, "Heat Transfer by Free Convection from Horizontal Cylinders to CO_2 under Near-Critical Conditions," *High Temperature*, vol. 11, part 1, pp. 524-528.